Theoret. chim. Acta (Berl.) 16, 1—21 (1970)

Commentationes

Hyperfine and Quadrupole Interactions at Nitrogen in Hemin*

P. S. HAN and T. P. DAS

Department of Physics, University of California, Riverside, California 92502

M. F. RETTIG

Department of Chemistry, University of California, Riverside, California 92502

Received April 11, 1969/August 8, 1969

The hyperfine and quadrupole coupling constants at nitrogen in iron (III) porphyrin chloride have been calculated. The wave functions were obtained by means of a self-consistent charge extended Hückel method [2]. The spin Hamiltonian for the system is

$$\mathscr{H} = A\boldsymbol{I}\cdot\boldsymbol{S} + \boldsymbol{I}\cdot\vec{\boldsymbol{B}}\cdot\boldsymbol{S} + \frac{e^2Qq_{z''z''}}{4I(2I-1)}[(3I_{z''}^2 - \boldsymbol{I}\cdot\boldsymbol{I}) + \eta(I_{x''}^2 - I_{y''}^2)]\,,$$

where the double-primed axis refers to the principal axis system of the field-gradient tensor. In the calculation of the nitrogen hyperfine constant, three contributions were considered: 1) the Fermi contact term; 2) the exchange polarization contribution; 3) the many body contribution. The last contribution was included because of its large relative importance in atomic nitrogen. The Fermi contact contribution dominates the nitrogen hyperfine constant, and the contact term has a 15% contribution from non-local effects, indicating significant unpaired electron density between iron and nitrogen. The exchange polarization term is negative and smaller than the Fermi contact term. Correlation effects are quite small, in contrast to the atomic nitrogen case. The dipolar hyperfine terms and the principal axis system of the hyperfine interaction were also evaluated. The quadrupole coupling constant for nitrogen was calculated, as well as the corresponding principal axis system. The contribution of unpaired electrons to the field gradient at nitrogen is substantial. The results of the calculations suggest considerable delocalization of unpaired electrons, in contrast to what one assumes using a crystal field model.

Die Hyperfein- und Quadrupol-Kopplungskonstanten für Stickstoff in Eisen(III) Porphyrinchlorid wurden ausgerechnet. Die Wellenfunktionen wurden mittels einer erweiterten Hückelmethode [2] — mit selbstkonsistenter Ladung — gewonnen. Der Spin-Hamiltonoperator für dies System ist:

$$\mathscr{H} = A\boldsymbol{I}\cdot\boldsymbol{S} + \boldsymbol{I}\cdot\vec{\boldsymbol{B}}\cdot\boldsymbol{S} + \frac{eQq_{z''z''}}{4I(2I-1)}[(3I_{z''}^2 - \boldsymbol{I}\cdot\boldsymbol{I}) + \eta(I_{x''}^2 - I_{y''}^2)]\,,$$

wobei die doppelt gestrichenen Koordinaten sich auf das Hauptachsensystem des Feldgradiententensors beziehen. Bei der Berechnung der Konstanten der Hyperfeinstruktur des Stickstoff wurden drei Beiträge berücksichtigt: 1. der Fermikontaktterm; 2. der Beitrag der Austauschpolarisation; 3. der Vielkörperbeitrag. Der letzte Beitrag wurde wegen seiner relativen Wichtigkeit beim atomaren Stickstoff mit eingeschlossen. Der Fermikontakt-Beitrag beherrscht die Hyperfeinkonstante des Stickstoffs, 15% des Beitrags vom Kontaktterm rühren von nichtlokalen Effekten her und deuten offensicht-

* Supported in part by the National Science Foundation and by the Petroleum Research Fund of the American Chemical Society.

lich auf eine Elektronendichte zwischen dem Eisen- und Stickstoffatom, die auf ungepaarte Elektronen hinweist. Der Term der Austauschpolarisation ist negativ und kleiner als der Fermikontaktterm. Korrelationseffekte sind ganz klein, im Gegensatz z. B. des atomaren Stickstoff. Die dipolaren Hyperfeinterme und das Hauptachsensystem der Hyperfeinwechselwirkung wurden ebenfalls ermittelt. Die Quadrupolkopplungskonstante für Stickstoff wurde ebenso errechnet wie das zugehörige Hauptachsensystem. Der Beitrag von ungepaarten Elektronen zum Feldgradienten beim Stickstoffatom ist wesentlich. Die Rechenergebnisse lassen eine bemerkenswerte Delokalisierung von ungepaarten Elektronen vermuten, im Gegensatz zu dem, was man erwartet, wenn man ein Kristallfeld-Modell benützt.

Calcul des constantes de couplage hyperfin et quadrupolaire sur l'azote dans le chlorure de porphyrine Fe(III). Les fonctions d'ondes ont été obtenues à l'aide d'une méthode de Hückel étendue itérative [2]. L'hamiltonien de spin du système est:

$$\mathscr{H} = A\boldsymbol{I}\cdot\boldsymbol{S} + \boldsymbol{I}\cdot\vec{\boldsymbol{B}}\cdot\boldsymbol{S} + \\ + \frac{e^2 Q q_{z''z''}}{4I(2I-1)}\left[(3I_{z''}^2 - \boldsymbol{I}\cdot\boldsymbol{I}) + \eta(I_{x''}^2 - I_{y''}^2)\right]$$

où les axes doublement indicés sont les axes principaux du tenseur gradient de champ. Trois contributions sont envisagées dans le calcul de la constante hyperfine sur l'azote: 1) le terme de contact de Fermi, 2) la polarisation d'échange, 3) le terme à N corps. Cette dernière contribution a été incluse à cause de son importance relative dans l'azote. Le terme de contact est dominant et contient 15% d'effets non locaux, ce qui indique une densité d'électron non apparié significative entre le fer et l'azote. Le terme de polarisation d'échange est négatif et plus petit que le terme de contact. Les effets de corrélation sont assez petits, contrairement au cas de l'azote atomique. Les termes hyperfins dipolaires et le système d'axe principal de l'interaction hyperfine ont aussi été évalués. La constante de couplage quadrupolaire pour l'azote a été calculée ainsi que l'axe principal correspondant. La contribution des électrons célibataires au gradient de champ sur l'azote est importante. Les résultats des calculs suggèrent une délocalisation considérable des électrons non appariés, contrairement à ce que l'on suppose lorsque l'on emploie un modèle de champ cristallin.

1. Introduction

In an earlier paper [1], the hyperfine field and quadrupole coupling constant for iron Fe^{57m} in hemin from Mössbauer data have been analyzed using molecular wavefunctions obtained by the extended Hückel approach [2]. These studies lend further support to the molecular orbital (MO) picture for optical properties of metalloporphyrins that has been developed by Gouterman [2], and Pullman [3] and their collaborators, but not all properties of the molecules are successfully calculated-notably the sign of the quadrupole splitting at iron [1].

The present paper is the second in our continuing series of investigations of the properties of hemin, and deals with the theory of magnetic hyperfine and electric quadrupole interaction of the ligand N^{14} nuclei. The purpose of this investigation is two-fold. First, magnetic resonance experiments on hemin and related compounds are currently in progress in several laboratories, and it would be desirable to have theoretical predictions both to assist in the experimental analysis and to compare with specific experimental results when these are available [4]. This work is expected to be a more critical test of the validity of MO theory than was the interpretation of Fe^{57m} Mössbauer data, because crystal field theory [5], which assumes the unpaired electrons to be associated with the iron atom alone, would lead to very feeble N^{14} hyperfine effects.

A second important reason for the prevent investigation is that the hyperfine interaction in the isolated nitrogen atom [6] arises entirely from exchange-

polarization and many body effects which are comparable in importance. This leads us to expect that such effects would also be important in hemin although the direct contribution to the N^{14} hyperfine constant is no longer expected to vanish as in the free nitrogen atom. A convenient procedure based on the Brueckner-Goldstone many-body perturbation [7] theory has recently been applied [6] to obtain a successful quantitative explanation of the hyperfine interaction in free nitrogen. We have adapted this procedure to the case of N^{14} nucleus in hemin using a pseudo-atom picture based on Mulliken's population analysis. While this procedure is applied here specifically to hemin, it should also be applicable to other nitrogen containing compounds.

The wave-functions are discussed in Section 2. Using these wave-functions, the contact interaction including manybody effects is discussed in Section 3, and the magnetic dipolar and quadrupole interactions are discussed in Section 4.

2. Electronic Wave Functions and Mulliken Population Analysis

The extended Hückel molecular orbitals ψ_μ are expressed as

$$\psi_\mu = \sum_i c_{\mu i} \varphi_i \tag{1}$$

where $c_{\mu i}$ is the coefficient of the i^{th} atomic orbital (AO) φ_i in the μ^{th} MO. The AO basis was chosen to be real, i.e., $p_x, p_y, \ldots d_{xz}, d_{xy}, \ldots$ On applying a variational procedure to obtain the $c_{\mu i}$ in Eq. (1), we obtain the linear equation

$$\sum_i c_{\mu i}(h_{ij} - \varepsilon_i S_{ij}) = 0, \quad j = 1, 2, \ldots, n \tag{2}$$

which leads to the secular determinant

$$|h_{ij} - \varepsilon S_{ij}| = 0 \tag{3}$$

with

$$h_{ij} = \langle \varphi_i | h | \varphi_j \rangle$$
$$S_{ij} = \langle \varphi_i | \varphi_j \rangle$$

h being the effective one-electron Hamiltonian. In the extended Hückel method the matrix elements h_{ij} and S_{ij} are taken over all the basis orbitals, both π and σ.

The secular determinant was constructed and solved by means of a modified version of Hoffmann's [8] original MO program. This method does not involve a complete self-consistent field calculation but instead provides charge self-consistency. It is thus referred to as a self-consistent charge (SCC) procedure [9].

In the extended Hückel calculation for iron (III) porphyrin chloride, we made use of the Wolfsberg-Helmholz [10] expression for the off-diagonal Hamiltonian matrix elements:

$$h_{ij} = \frac{K}{2}(h_{ii} + h_{jj}) S_{ij}. \tag{4}$$

The diagonal elements of $\mathscr{H}$ were obtained [2] by means of Eq. (5):

$$h_{ii} = (h_{ii}^{\pm} - h_{ii}^{0}) q_l + h_{ii}^{0}. \tag{5}$$

We utilized the same cartesian coordinates, overlap integrals S_{ij} and $K = 1.89$ as was done by Zerner, Gouterman, and Kobayashi (ZGK, [2]). The values of S_{ij} were obtained by ZGK using single exponential functions adjusted to fit the tails of actual *atomic* SCF functions. For subsequent calculation [1] of hyperfine properties, the actual SCF orbitals [11] φ_i were utilized. The quantities q_l in Eq. (5) represent atomic charge densities which are obtained by the Mulliken population analysis procedure [12, 13]:

$$q_l = \sum_{\mu} \sum_{i} \left[|c_{\mu i}^{l}|^2 + \sum_{m \neq l} \sum_{j} (c_{\mu i}^{l} c_{\mu j}^{m} S_{ij}) \right] n(\mu) - Z_l \,. \tag{6}$$

In Eq. (6), the sum over i refers to the atomic orbitals on atom l, while the sum over j refers to the atomic orbitals on atom m. The sum over μ refers to the molecular orbitals with $n(\mu) = 0$, 1, 2 depending on whether the particular MO is empty, singly or doubly occupied. The parameters $h_{ii}^{\pm}$ and h_{ii}^{0} were obtained from spectroscopic data [2]. These parameters were chosen to have different values for different orbitals (i) on the same atom (l). The last term in Eq. (6), namely Z_l refers to the core-charge on the l^{th} atom (that is, charge after the removal of valence electrons).

The molecular geometry and coordinate axis system are shown in Fig. 1. The atomic orbitals included in these calculations were the $2s$ and $2p$ orbitals on the carbon and nitrogen atoms, $3s$ and $3p$ on chlorine, $1s$ on hydrogen and $3d$, $4s$, and $4p$ on iron. These added up to a total of 121 orbitals, so that the summation in μ in Eq. (6) extends nominally over 121 MO's, although actually a number of the higher ones drop out because $n(\mu) = 0$ for them.

There are two minor differences between the procedure we followed and that of ZGK [2].

1. We did not make use of the molecular symmetry in factoring the secular equation, but instead used the predictions of group theory as a check on the wave-functions resulting from our calculations.

2. The solution of the secular Eq. (3) using the matrix elements in Eqs. (4) and (5) by the SCC procedure requires an iteration of q_i. Our method of arriving at this charge convergence was slightly different. We arrived at the atomic charges for the λ^{th} iteration by means of a weighted average of the calculated (or guessed) input charges and output charges for the $(\lambda - 1)^{\text{th}}$ iteration:

$$q_{l,\,\text{input}}^{\lambda} = \frac{w q_{l,\,\text{input}}^{\lambda-1} + q_{l,\,\text{output}}^{\lambda-1}}{w+1} \,. \tag{7}$$

For the convergence parameter w in Eq. (7), we used the value $w = 10$ and iterations were continued until the condition

$$|q_{l,\,\text{input}}^{\lambda-1} - q_{l,\,\text{output}}^{\lambda-1}| \leqq 0.05$$

was satisfied for all 38 atoms. When this condition is satisfied, a final set of charges is generated according to Eq. (7), and a final interaction is carried out.

The strategy of the calculation was the same as that of ZGK, where the five unpaired electrons ($n(\mu) = 1$) in the summation (6) were restricted to molecular orbitals which are predominantly made up of iron $3d$ orbitals. This is a justifiable procedure since the extended Hückel method does not consider exchange

Table 1

Atom	AO	Atomic orbital charges	
		paired	unpaired
2	$2s$	1.3359	0.0082
2	$2p_z$	1.2784	0.0419
2	$2p_x$	1.1156	0.0033
2	$2p_y$	1.1907	0.1945

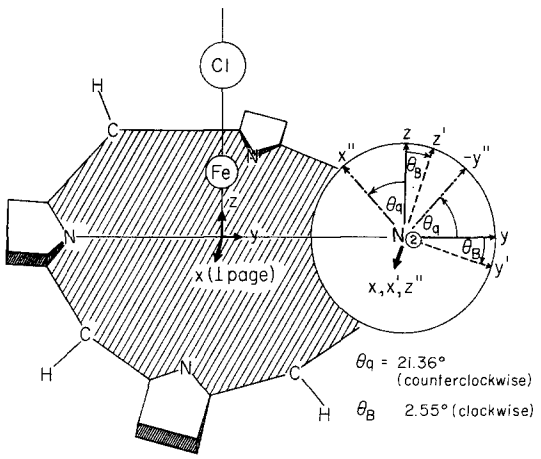

Fig. 1. Molecular geometry of iron (III) porphyrin chloride and principal axis systems: ———, molecular axes; – – – –, principal axes of $\vec{B}$ — · — · —, principal axes of $\vec{q}$. The axis ⊥ to the page is the axis of rotation in going from the molecular axis system to the principal axis systems. Thus only the cartesian axes in the plane of the paper change their spatial orientation (Part of the right-hand pyrrole ring is deleted for clarity)

effects. A more complete calculation including exchange effects is expected [2] to lead to the ground state which has been used here. The calculated results are nearly identical to those of ZGK, the only significant change being slight differences in atomic charges brought about by the different method of charge covergence. Since our calculated orbital charges are within 3% of ZGK's results and our calculated MO energies are within ± 0.2 eV of theirs, we do not present extensive tabulations of our results.

Table 1 presents the Mulliken population analysis results for the nitrogen atom labelled 2 in Fig. 1. From the data in Table 1, we calculated for the nitrogen "pseudo-atom" electronic configuration:

$$(2s)_\alpha^{0.67615}\,(2s)_\beta^{0.66795}\,(2p)_\alpha^{2.0320}\,(2p)_\beta^{1.7923}\,.$$

Thus, for example, the $(2p)_\alpha$ configuration is obtained as one half the sum of the $2p_x$, $2p_y$, $2p_z$ paired orbital charges plus the sum of the unpaired contributions. The $(2p)_\beta$ contribution, on the other hand, is just one half the sum of the paired orbital charges. These "pseudo-atom" results will be used in Section 3 in the calculation of the exchange-polarization and many-body effects in the N^{14} hyperfine constants.

3. Theory of N^{14} Contact Interaction

The isotropic hyperfine interaction arises from the Fermi contact Hamiltonian [14]:

$$\mathscr{H}_F = \frac{8\pi}{3}\gamma_e\gamma_{N^{14}}\hbar^2\sum_k \boldsymbol{I}\cdot\boldsymbol{s}_k\delta(\boldsymbol{r}_k) \tag{8}$$

where $\gamma_e = g_e\beta_e/\hbar$ and $\gamma_{N^{14}} = g_N\beta_N/\hbar$ are gyromagnetic ratios; g_e and g_N are the g-factors for the electron and nucleus and β_e and β_N are the Bohr magneton and nuclear magneton.

If the exact many-electron wave-function for the molecule were available, the hyperfine energy would be obtained by taking the expectation value of $\mathscr{H}_F$ over this wave-function. Unfortunately one usually works with the one-electron approximation to the many-electron wave-function where many body correlation effects [6] are missing. In addition, the one-electron approximation to the wave-function often lacks the exchange polarization effect [15] which makes the wave-function of paired states with spin parallel to the unpaired valence orbitals different from those with spin anti-parallel. One thus has to explicitly include these contributions to the hyperfine constant when utilizing MO wave-functions for the calculation.

Summarizing, there are three distinct contributions that have to be considered in the calculation of the hyperfine constant. First, there is the direct constribution arising from the finite expectation value of $\mathscr{H}_F$ over the unpaired valence orbitals. Secondly, one has to consider the exchange polarization contribution arising from the exchange interaction of the paired valence electrons and the paired core electrons with the unpaired valence electrons. Thirdly, there is the many-body contribution arising from the instantaneous correlation between the paired and unpaired electrons, which is neglected in one electron theory.

The role of correlation and exchange polarization effects is particularly pronounced in the free nitrogen atom, due to the vanishing direct contribution from the unpaired p-electrons. The exchange polarization contribution is a combination [6] of nearly equal effects of opposite sign from the $1s$ and $2s$ cores namely -49.711 mHz and $+55.419$ mHz, respectively. The net exchange polarization result is thus $+5.708$ mHz as compared to the experimental result [16] of $+10.45 \pm 0.00007$ mHz.

The remainder of the observed hyperfine coupling arises from correlation effects and a small additional contribution from consistency effects [6] associated with the exchange-polarization. The major many-body effects has been found to arise from correlation between the $2p$ orbitals and the $1s$ and $2s$ orbitals. The correlation among the unpaired $2p$ orbitals was found to have a vanishing effect on the hyperfine constant. These results were arrived at by the Brueckner-Goldstone many-body diagrammatic technique [7]. In studying exchange-polarization and correlation effects in hemin, we shall make use of as suitable adaption of this many-body procedure as applied to free atoms.

The direct contribution to the N^{14} hyperfine constant in hemin can be calculated in a straightforward manner by taking the expectation value of $\mathscr{H}_F$ over the molecular wave-function with the delta function centered at the nitrogen site. In the molecular orbital theory, the expectation values refer to the

individual molecular orbitals. In the RHF approximation, where the orbital parts of the paired states are the same, the expectation value of the hyperfine Hamiltonian reduces to a sum over only the unpaired orbitals. Thus the direct part of the parameter A in the spin Hamiltonian $A\boldsymbol{I}\cdot\boldsymbol{S}$ is given by

$$\begin{aligned} A_{\text{direct}} &= \frac{8\pi\gamma_e\gamma_{N^{14}}\hbar^2}{6S} \sum_{\substack{\mu \\ \text{unpaired MO's}}} |\psi_\mu(\mathrm{N})|^2 \\ &= -524 \sum_{\substack{\mu \\ \text{unpaired MO's}}} |\psi_\mu(\mathrm{N})|^2 \quad (\mathrm{kG}) \\ &= 64.483 \sum_{\substack{\mu \\ \text{unpaired MO's}}} |\psi_\mu(\mathrm{N})|^2 \quad (\mathrm{mHz}) \end{aligned} \tag{9}$$

where

$$\begin{aligned} \sum_\mu |\psi_\mu(\mathrm{N})|^2 &= \sum_\mu |c^{\mathrm{N}}_{\mu,2s}|^2 \, |\varphi_{2s}(\mathrm{N})|^2 \\ &\quad + \sum_\mu \sum_i \left(c^{\mathrm{N}}_{\mu,2s} c_{\mu i} \varphi_{2s}(\mathrm{N})\, \varphi_i(\mathrm{N}) + |c_{\mu i}|^2 \, |\varphi_i(\mathrm{N})|^2\right) \end{aligned} \tag{10}$$

and the orbitals i refer to atoms other than the nitrogen atom under consideration. The three terms inside the bracket in Eq. (10) can be interpreted as representing local, non-local, and distant contributions, respectively. The values were obtained for these quantities with the MO wave-functions are:

$$A^{\text{local}}_{\text{direct}} = 4.8436 \text{ mHz}, \tag{11a}$$

$$A^{\text{non local}}_{\text{direct}} = 0.8103 \text{ mHz}, \tag{11b}$$

$$A^{\text{distant}}_{\text{direct}} = 0.0030 \text{ mHz}. \tag{11c}$$

The fact that the non-local contribution is significant, though smaller than the local contribution, indicates that there is substantial distribution of the unpaired electrons in the region between iron and nitrogen atoms, in contrast to what would be expected for the extreme ionic picture of the crystal-field model [5].

We turn next to the contribution to the nitrogen hyperfine constant from the exchange and correlation between the unpaired electrons and the paired electrons in the molecule. The latter include both the paired MO and the core electrons. Ideally one would want to calculate the exchange-polarization and correlation effects using the actual MO wave-functions for the molecule. For the exchange-polarization effect this could be done by the unrestricted Hartree-Fock (UHF) method [17]. The latest adaptation of this method to molecular calculations has been presented by Pople [18] using the INDO approach. An alternate procedure, if the paired electrons are localized even though the unpaired ones may be delocalized, is to make use of the moment-perturbation (MP) method [19] that has been used in solid state calculations. However, as we have seen in the case of the free nitrogen atom, it is quite likely that the influence of correlation on the hyperfine constant may be comparable to the exchange-polarization effect. To handle the correlation effect in the framework of current molecular orbital methods, one would have to employ a configuration interaction procedure, involving addition of configurations in which some of the electrons occupy higher orbitals. In our present work, however, we shall utilize an adaptation of the

Brueckner-Goldstone many-body procedure for atoms, which allows us to deal with both exchange-polarization and correlation contributions by similar analyses involving diagrammatic perturbation theory.

A detailed description of the Brueckner-Goldstone many-body theory, as applied to atoms, can be found in a number of places [6, 7]. We want to present here only a few bare essentials to explain our adaptation of the results for the nitrogen atom with this theory to obtain approximate results for the nitrogen nucleus for hemin. The Brueckner-Goldstone theory involves essentially a perturbation approach, the relevant perturbation being the difference between the actual Hamiltonian such as the Hartree-Fock Hamiltonian. Thus the Hamiltonian for a many-electron system is given by

$$\mathscr{H} = \sum_i T_i + \sum_{i>j} \frac{1}{r_{ij}} \tag{12}$$

where T_i is the kinetic energy and the nuclear coulomb potential operator for the i^{th} electron,

$$T_i = -\frac{1}{2} V_i^2 - \frac{Z}{r_i}. \tag{13}$$

The zero-order Hamiltonian chosen can be expressed as

$$\mathscr{H}_0 = \sum_i (T_i + V_i) \tag{14}$$

where V_i is a combination of usual coulomb and exchange potential between electrons in Hartree-Fock theory. The perturbation is given by

$$\mathscr{H}' = \sum_{i>j} \frac{i}{r_{ij}} - \sum_i V_i \tag{15}$$

If Φ_0 is to represent the eigenfunction of $\mathscr{H}_0$, then according to the Brueckner-Goldstone perturbation theory, the correct eigenfunction Ψ_0 of $\mathscr{H}$ is given by

$$\begin{aligned} \Psi_0 &= \sum_{n=0}^{\infty}{}_L \left(\frac{1}{E_0 - \mathscr{H}_0} \mathscr{H}' \right)^n \Phi_0 \\ &= \Phi_0 + \Phi^{(1)} + \Phi^{(2)} + \cdots + \Phi^{(n)} + \cdots \end{aligned} \tag{16}$$

where L means that only linked terms are included. The meaning of this will be clear when we draw the diagrams. The perturbed function $\Phi^{(1)} + \Phi^{(2)} + \cdots + \Phi^{(n)} + \cdots$ can be obtained from the perturbation expansion by introducing the unity operator in terms of the projection operators P_m namely,

$$\mathbf{1}_{\text{op.}} = \sum_m P_m = \sum_m |\Phi_m\rangle \langle \Phi_m| \tag{17}$$

where the $|\Phi_m\rangle$ form a complete set of states obtained from single, double, triple, etc., excitations from the ground state Φ_0. The single particle excited state wave functions φ_i are eigenfunctions of the single particle equations

$$(T + V)\, \varphi_i = \varepsilon_i \varphi_i \tag{18}$$

where i refers to a state other than the lowest ones which are occupied for the unperturbed determinantal state Φ_0.

The hyperfine constant can now be obtained by taking the expectation value of the hyperfine Hamiltonian in Eq. (8) over the corrected wave function Ψ_0. Thus,

$$A = \frac{16\pi}{3} \frac{\beta \mu_{N^{14}}}{IS} \frac{\langle \Psi_0 | \not{f} | \Psi_0 \rangle}{\langle \Psi_0 | \Psi_0 \rangle} \tag{19}$$

where $\not{f} = \sum_i \delta(\boldsymbol{r}_i)\, s_{zi}$.

On substituting for Ψ_0 from Eq. (16), we obtain

$$\langle \Psi_0 | \not{f} | \Psi_0 \rangle = f_{00} + 2f_{01} + f_n + 2f_{02} + \cdots + 2f_{mn} + \cdots \tag{20}$$

where $f_{mn} = \langle \Phi^{(m)} | \not{f} | \Phi^{(n)} \rangle$.

In earlier work on atomic problems using Brueckner-Goldstone many-body theory, it has been shown [6, 7] that a convenient procedure to handle quantities like f_{mn} is to use a diagrammatic procedure similar to that in quantum electrodynamics. The reader is referred to these earlier papers [6, 7] for a detailed description of the procedure for drawing Feynman-like diagrams in Brueckner-Goldstone theory.

A typical (0,1) diagram which describes the exchange polarization effect in nitrogen atom is shown in Fig. 2. The line on the left-hand side represents [7] a "hole" $1s$ line, meaning thereby a $1s$ state that has been left vacant by an electron that is excited by exchange with a $2p$ electron to a higher ks-state ($k > 2$ or continuum) the latter being referred to as a particle ks line. The vertices ·---· and ~~~~· are associated with operators $\mathscr{H}'$ and $\not{f}$, respectively. In algebraic terms, the contribution of this diagram is given by

$$\delta E = -\frac{8\pi}{3} \gamma_e \gamma_{N^{14}} \hbar^2 \left(\frac{I}{2}\right) \times \frac{\langle \varphi_{2p}(1)\varphi_{ks}(2)| \dfrac{1}{r_{12}} |\varphi_{1s}(1)\varphi_{2p}(2)\rangle \langle \varphi_{1s}(1)|\, \delta(\boldsymbol{r})\, |\varphi_{ks}(1)\rangle}{\varepsilon_{1s} - \varepsilon_{ks}}. \tag{21}$$

Another typical diagram of the (1,1) type, is shown in Fig. 3. This diagram represents the effect on the hyperfine constant of the correlation between $2p$ and $1s$ states leading to the excitation of an electron in the $2p$ state to higher $k's$ and $k''s$ states. The superfices $\pm$ indicate up or down spin states, that is, spins parallel or antiparallel to those of the unpaired electrons. The hyperfine energy associated with this diagram is given by

$$\delta E = \frac{8\pi}{3} \gamma_e \gamma_{N^{14}} \hbar^2 \left(\frac{I}{2}\right) \times \frac{\langle \varphi_{kp}(1)\varphi_{k's}(2)| \dfrac{1}{r_{12}} |\varphi_{1s}(1)\varphi_{2p}(2)\rangle}{(\varepsilon_{1s} + \varepsilon_{2p} - \varepsilon_{kp} - \varepsilon_{k's})} \times \frac{\langle \varphi_{1s}(1)\varphi_{2p}(2)| \dfrac{1}{r_{12}} |\varphi_{kp}(1)\varphi_{k''s}(2)\rangle \langle \varphi_{k''s}(1)|\, \delta(\boldsymbol{r}_1)\, |\varphi_{k's}(1)\rangle}{(\varepsilon_{1s} + \varepsilon_{2p} - \varepsilon_{kp} - \varepsilon_{k''s})}. \tag{22}$$

A typical (0,2) diagram is indicated in Fig. 4. It represents the combined effects of correlation and exchange polarization. Thus, the $1s^-$ and $1s^+$ states

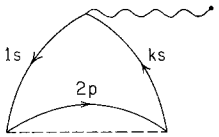

Fig. 2. Exchange polarization diagram

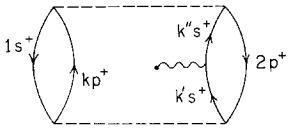

Fig. 3. Typical (1,1) type diagram

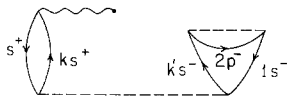

Fig. 4. (0,2) Type correlation diagram

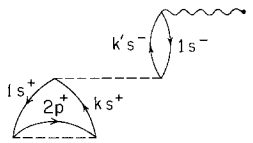

Fig. 5. Consistency diagram

may be considered to mutually perturb each other by correlation, the perturbed ks^+ state returning to the ground $1s^+$ state via the hyperfine interaction. The $k's^-$ state, associated with the perturbed $1s^-$ state, is de-excited back to the ground $1s^-$ state by exchange with the $2p^-$ electron. The hyperfine energy associated with this diagram is given by:

$$\delta E = -\frac{8\pi}{3}\gamma_e\gamma_{N^{14}}\hbar^2\left(\frac{I}{2}\right) \times \langle\varphi_{ks}(1)\varphi_{k's}(2)|\frac{1}{r_{12}}|\varphi_{1s}(1)\varphi_{1s}(2)\rangle \times \frac{\langle\varphi_{2p}(1)\varphi_{1s}(2)|\frac{1}{r_{12}}|\varphi_{k's}(1)\varphi_{2p}(2)\rangle\langle\varphi_{1s}(1)|\delta(\boldsymbol{r}_1)|\varphi_{ks}(1)\rangle}{(2\varepsilon_{1s}-\varepsilon_{k's}-\varepsilon_{ks})(\varepsilon_{1s}-\varepsilon_{k's})}. \tag{23}$$

The hyperfine energies obtained from all these diagrams can be converted into contributions to hyperfine constants using the relation

$$A = \frac{\delta E}{IS}$$

where S is the total electronic spin of the atom, 3/2 for nitrogen. The contributions from the (0,1), (1,1) and (0,2) diagrams to the hyperfine constant [6] for nitrogen atom are listed in Table 2 and add up to a value quite close to the experimental result. The (1,1) and (0,2) diagrams represent mainly the correlation effect except for diagrams of the type shown in Fig. 5, which are one-electron in nature and represent consistency contributions to the exchange-polarization effect from the (0,1) diagram in Fig. 2. The hyperfine energy of this consistency diagram is given by:

$$\delta E = -\frac{8\pi}{3}\gamma_e\gamma_{N^{14}}\hbar^2\left(\frac{I}{2}\right) \times \langle\varphi_{2p}(1)\varphi_{ks}(2)|\frac{1}{r_{12}}|\varphi_{1s}(1)\varphi_{2p}(2)\rangle \times \frac{\langle\varphi_{1s}(1)\varphi_{k's}(2)|\frac{1}{r_{12}}|\varphi_{ks}(1)\varphi_{1s}(2)\rangle\langle\varphi_{1s}(1)|\delta(\boldsymbol{r}_1)|\varphi_{k's}(1)\rangle}{(\varepsilon_{1s}-\varepsilon_{ks})(2\varepsilon_{1s}-\varepsilon_{ks}-\varepsilon_{k's})}. \tag{24}$$

Table 2. *Net contributions from all (0,1), and (1,1) and (0,2) diagrams*

Class of diagram	Contribution mHz
(0,1)	5.70810
(1,1)	5.20194
(0,2)	− 0.39760
Total	10.51243
Experiment	10.45 ± 0.00007

We shall next consider the adaptation of the diagrams for the nitrogen atom to evaluate the exchange-polarization and many-body contributions to the N^{14} hyperfine constant in hemin. In a straightforward extension of the many-body perturbation method to study hyperfine interaction in a molecule such as hemin, one would again have to deal with diagrams similar to those indicated in Figs. 2–5. However, the hole and particle lines in these diagrams would now involve multicenter wave-functions which could be rather difficult to handle. One has, therefore, to resort to approximation, and in this connection a "pseudo-atom" picture can be utilized to advantage. The procedure we have adopted is to continue to use the diagrams for the free atom but weight their contributions by appropriate factors depending on the populations in the various electronic states of the nitrogen "pseudo-atom" in hemin.

We start by considering the exchange-polarization diagram in Fig. 2. From the population distribution listed in Table 1 for the pseudo-atom, we notice that there are now 0.2396 unpaired $2p$-electrons which polarize the $1s$ electrons, in contrast to three unpaired $2p$-electrons in the free atom. In addition, one has to take into account the difference in the spins of nitrogen atom and hemin of $S = 3/2$ and 5/2, respectively. Thus, the $1s$ contribution for the atom has to be multiplied by a factor:

$$A = \frac{0.2396}{3} \times \frac{3}{5}.$$

For the exchange-polarization effect associated with $2s$ state, there is an additional factor to be considered since the $2s$ population in each spin state is now about 0.668 in place of unity as it was in the free atom. The conversion factor for the $2s$ contribution is then

$$B = A \times 0.668 .$$

These factors are utilized in obtaining the exchange-polarization contribution listed in Table 4. In Fig. 3, the hole line on the left can be $1s^{\pm}$ or $2s^{\pm}$. Since the hyperfine vertex is attached to the particle line associated with the perturbation of the $2p$ states, the contribution to the hyperfine structure again depends upon the difference in up and down spin populations for the $2p$ states. It then appears that the conversion factors to get "pseudo-atom" results are again respectively A and B for the $1s$ and $2s$ states. The conversion factors for Fig. 4 are exactly the same as those of Fig. 2 and Fig. 3 as long as both hole lines do not refer to the $2s$ state. In this latter case the conversion factor involves the factor given by:

$$C = A \times (0.668)^2 .$$

Table 3

Figure	Atomic contributions, mHz		Conversion factors for "pseudo-atom"		pseudo atom *hfs* mHz	
	1*s* state	2*s* state	1*s* state	2*s* state	1*s* state	2*s* state
2	−50.430	+56.220	*A*	*B*	−2.41557	1.78811
3	0.28695	1.51351	*A*	*B*	0.01374	0.04495
4	− 0.610142	1.97335	*A*	*C*	−0.02922	0.04167
5	− 1.59135	4.77559	*A*	*C*	−0.07622	0.10085

Table 4. *Nitrogen "Pseudo-Atom" hfs in Hemin*

Order of contribution	Description	*hfs constant, mHz*
(0,0)	direct	5.6569
(0,1)	exchange-polarization	−0.6242
(1,1)	correlation	0.1706
(0,2)	correlation and consistency	−0.1035
Total		5.0998
		(= 1.82 gauss[a])

[a] A (gauss) = A (mHz) $(g_e/g)/2.80$.

An inspection of Fig. 5 indicates the conversion factors for the "pseudo-atom" are the same as in Fig. 4. These considerations have yielded the entries in Table 3 for the contribution of Figs. 2–5.

The same conversion procedure has been applied to all the diagrams for nitrogen atom leading to the net (0,1), (1,1) and (0,2) contributions in Table 4.

The (0,1) contribution represents the effects of the exchange-polarization which is the next important contributor after the (0,0) direct effect. There could be an additional small exchange-polarization contribution from the influence of the small 0.0082 surplus population in the 2*s* up spin states on the 1*s* cores. This effect is not taken into account in our diagrams. However, we have evaluated this contribution by the moment-perturbation procedure [19] and found a negligible value, 0.0033 mc/sec. The combined effect of (1,1) and (0,2) diagrams represents the sum-total of the influence of many-body effects and is seen to be small compared to the exchange-polarization effect. While this net contribution from many-body effects is a small fraction of other effects, the former arises out of the differences of large numbers from individual diagrams and it would have been impossible to ascertain its magnitude without actual calculation.

Two main criticisms could be raised about the adaptation procedure used to derive the hyperfine constant in hemin from that for the free atom. The first has to do with the use of the "pseudo-atom" population in the weighting factors utilized. This could be construed as equivalent to the assumption that the total contribution to each diagram arises from electrons in the neighborhood of the nitrogen atom rather than the entire region spanned by the pertinent molecular orbitals. This criticism is however not entirely justified since the Mulliken population analysis is an attempt to describe the delocalized nature of the electronic

distribution. Further, the major part of the direct hyperfine structure contribution has been found earlier in this section to arise from the orbital density on the nitrogen atom alone. Only about 15% of the direct hyperfine structure arises from the nonlocal term involving iron $3d$ orbital. The exchange-polarization and many-body correlation contributions to the hyperfine structure are expected to be even more short range in nature than the direct hyperfine interaction. Thus, we expect only about 10% error in our estimation exchange-polarization and many-body effects due to the use of "pseudo-atom" technique.

The second possible criticism is the use of the same excited state energies and wave functions in the diagrams for the "pseudo-atom" as in the atomic case. This criticism may be answered by noting that for most of the important diagrams, the major contribution [6] arises from the continuum excited states and these are not expected to be bery sensitive to the difference in the potential for the "pseudo-atom" and the free atom.

The final calculated value of A is 1.82 gauss, and this may be compared with the result recently obtained by Scholes [4] for the nitrogen hyperfine splitting in hemin: 3.1 gauss. Scholes doped hemin (and hematin) into perylene and obtained well resolved *esr* spectra at 4.2 °K. Crystal orientation studies revealed a small ($<10\%$) dipolar contribution to the observed nitrogen hyperfine constant. Thus, we may consider that the experimental 3.1 gauss arises from the Fermi contact term. Our calculated result is about 60% of the experimental finding, which is acceptable agreement in view of the approximations involved.

We now consider the magnetic dipolar hyperfine tensor $\vec{\boldsymbol{B}}$.

4. Magnetic Dipole and Electric Quadrupole Coupling Constants

The electron-nuclear spin dipolar Hamiltonian is given by Eq. (25):

$$\mathscr{H}_{\text{dip}} = \gamma_e \gamma_{N^{14}} \hbar^2 \sum_i \frac{3(\boldsymbol{s}_i \cdot \boldsymbol{r}_i)(\boldsymbol{I} \cdot \boldsymbol{r}_i) - r_i^2 (\boldsymbol{s}_i \cdot \boldsymbol{I})}{r_i^5} \tag{25}$$

where γ_e and $\gamma_{N^{14}}$ are the gyromagnetic ratios of the electron and the N^{14} nucleus, I is the N^{14} nuclear spin, $\boldsymbol{r}_i$ is the vector from the origin at the nucleus to the i^{th} electron, and $\boldsymbol{s}_i$ is the spin of the i^{th} electron.

The contribution of $\mathscr{H}_{\text{dip}}$ to the spin-Hamiltonian will be given by:

$$\mathscr{H}_{\text{dip}}^{\text{spin}} = \boldsymbol{I} \cdot \vec{\boldsymbol{B}} \cdot \boldsymbol{S}. \tag{26}$$

The components of the tensor $\vec{\boldsymbol{B}}$ are obtained as usual by equating the matrix elements of $\mathscr{H}_{\text{dip}}$ over the total wavefunction to the matrix elements of $\mathscr{H}_{\text{dip}}^{\text{spin}}$ over the spin-function only, namely,

$$\langle \Psi | \mathscr{H}_{\text{dip}} | \Psi \rangle = \langle \chi | \mathscr{H}_{\text{dip}}^{\text{spin}} | \chi \rangle \tag{27a}$$

where

$$\Psi = \Phi \chi \tag{27b}$$

with

$$\Phi = |\psi_1(1)\, \psi_2(2)\, \psi_3(3)\, \psi_4(4)\, \psi_5(5)| \tag{27c}$$

and

$$\chi = \alpha(1)\,\alpha(2)\,\alpha(3)\,\alpha(4)\,\alpha(5)\,. \tag{27d}$$

The $\psi_n(n)$ in Eq. (27c) are the spatial parts of the one-electron MO's in Eq. (1), obtained from the extended Hückel calculation. As is usual with magnetic effects, only the half filled MO's have to be considered. Using this procedure, the components of the tensor $\vec{B}$ are given by:

$$\vec{B} = \begin{pmatrix} B_{xx} & B_{xy} & B_{xz} \\ B_{yx} & B_{yy} & B_{yz} \\ B_{zx} & B_{zy} & B_{zz} \end{pmatrix}$$

$$= \frac{\gamma_e \gamma_{N^{14}} \hbar^2}{5} \sum_{\substack{\mu \\ \text{unpaired} \\ \text{MO's}}} \sum_i \sum_j c_{\mu i} c_{\mu j} \langle \varphi_i | \frac{1}{r^3} \begin{pmatrix} \frac{3x^2 - r^2}{r^5} & \frac{3xy}{r^5} & \frac{3xz}{r^5} \\ \frac{3yx}{r^5} & \frac{3y^2 - r^2}{r^5} & \frac{3yz}{r^5} \\ \frac{3zx}{r^5} & \frac{3zy}{r^5} & \frac{3z^2 - r^2}{r^5} \end{pmatrix} | \varphi_j \rangle\,. \tag{28}$$

In the evaluation of $\vec{B}$ from Eq. (28), only the one-center local terms were retained. The two-center non-local and distant terms were neglected because of the sharp decay of the $1/r^3$ term as distance increases from the origin. This leads [20] to rather small values for the two-center integrals. The calculation for $\vec{B}$ was carried out for the nitrogen atom labelled 2 in Fig. 1. From symmetry considerations, the corresponding tensor for other ligand nitrogens can be obtained by rotational transformations. On retaining only the local terms, Eq. (29) for $\vec{B}$ reduced to

$$\vec{B} = \frac{\gamma_e \gamma_{N^{14}} \hbar^2}{5} \left\langle \frac{1}{r^3} \right\rangle_{2p} \sum_{\substack{\mu \\ \text{unpaired} \\ \text{MO's}}} \begin{pmatrix} \frac{2}{5}(2c_{\mu x}^2 - c_{\mu y}^2 - c_{\mu z}^2) & \frac{6}{5} c_{\mu x} c_{\mu y} & \frac{6}{5} c_{\mu x} c_{\mu z} \\ \frac{6}{5} c_{\mu y} c_{\mu x} & \frac{2}{5}(2c_{\mu y}^2 - c_{\mu z}^2 - c_{\mu x}^2) & \frac{6}{5} c_{\mu y} c_{\mu z} \\ \frac{6}{5} c_{\mu z} c_{\mu x} & \frac{6}{5} c_{\mu z} c_{\mu y} & \frac{2}{5}(2c_{\mu z}^2 - c_{\mu x}^2 - c_{\mu y}^2) \end{pmatrix} \tag{29}$$

where $c_{\mu x}$, $c_{\mu y}$, and $c_{\mu z}$ are the coefficients of the p_x, p_y and p_z atomic orbitals in the μ^{th} molecular orbital. The expectation value of $1/r^3$ over the $2p$-orbitals, namely $\langle r^{-3} \rangle_{2p} = 3.0996\, a_0^{-3}$, was obtained using the atomic SCF functions of Clementi [11] for the ^4S state. The numerical factors in Eq. (29) result from the angular integrations over p-orbitals.

Eq. (29) indicates, as expected, that $\vec{B}$ is identically zero in the free nitrogen atom since all the diagonal and off-diagonal elements vanish as a consequence of the spherical symmetry of the atom. In the molecule, the unequal populations of p_x, p_y, and p_z orbitals permits the elements of $\vec{B}$ to be non-vanishing. The off-diagonal elements B_{xy}, B_{yx}, B_{xz}, and B_{zx} vanish as a result of reflection

symmetry. The final result for $\vec{B}$ is in a non-diagonal representation corresponding to the molecular coordinate system in Fig. 1, is given by:

$$\vec{B} = \frac{\gamma_e \gamma_{N^{14}} \hbar^2}{5} \begin{pmatrix} -0.3374 & 0.0 & 0.0 \\ 0.0 & 0.5020 & -0.0296 \\ 0.0 & -0.0296 & -0.1646 \end{pmatrix}. \tag{30}$$

In order to transform $\vec{B}$ to a diagonal form it is necessary to rotate about the x-axis by an angle θ_B (see Fig. 1). The transformation matrix is expected to have the form:

$$\begin{pmatrix} c_{\mu x'} \\ c_{\mu y'} \\ c_{\mu z'} \end{pmatrix} = \begin{pmatrix} 1 & 0 & 0 \\ 0 & \cos\theta_B & \sin\theta_B \\ 0 & -\sin\theta_B & \cos\theta_B \end{pmatrix} \begin{pmatrix} c_{\mu x} \\ c_{\mu y} \\ c_{\mu z} \end{pmatrix}. \tag{31}$$

We seek a principal axis system in which the remaining off-diagonal elements vanish, that $B_{y'z'} = B_{z'y'} = 0$. This is equivalent to the condition:

$$\sum_{\substack{\mu \\ \text{unpaired} \\ \text{MO's}}} (c_{\mu y'} c_{\mu z'}) = 0. \tag{32}$$

Using Eqs. (31) and (32) we obtain

$$\sum_{\substack{\mu \\ \text{unpaired} \\ \text{MO's}}} c_{\mu y'} c_{\mu z'} = \text{Cup}(yz)\cos 2\theta_B + \frac{\text{Cup}(zz) + \text{Cup}(yy)}{2} \sin 2\theta_B = 0 \tag{33}$$

where $\text{Cup}(yz) = \sum_{\substack{\mu=1 \\ \text{unpaired} \\ \text{MO's}}}^{5} c_{\mu y} c_{\mu z}$. etc.

Eq. (32) leads to $\theta_B = -2.55°$, the negative sign indicating clockwise-rotation in Fig. 1, and the principal components of the dipolar hyperfine tensor $\vec{B}'$ are given by:

$$\vec{B}' = \frac{\gamma_e \gamma_{N^{14}} \hbar^2}{5} \begin{pmatrix} -0.3374 & 0.0 & 0.0 \\ 0.0 & 0.5059 & 0.0 \\ 0.0 & 0.0 & -0.1685 \end{pmatrix} \tag{34a}$$

$$= \begin{pmatrix} -2.5970 & 0.0 & 0.0 \\ 0.0 & 3.8941 & 0.0 \\ 0.0 & 0.0 & -1.2971 \end{pmatrix} \text{(mHz)}. \tag{34b}$$

It is sometimes convenient to express the components of hyperfine tensor $\vec{B}'$ in terms of the field $\boldsymbol{H}_{\text{nuc.}}$ at the nuclear site for *nmr* experiments, or in terms of $\boldsymbol{H}_{\text{elect.}}$, the field at the electron site in *esr* experiments. The two alternative forms of $\vec{B}'$ are given by

$$\boldsymbol{H}_{\text{nuc.}} = -\frac{\vec{B}' \cdot \boldsymbol{S}}{\gamma_{N^{14}} \hbar}, \tag{35a}$$

$$\boldsymbol{H}_{\text{elect.}} = \frac{\boldsymbol{I} \cdot \vec{B}'}{\gamma_e \hbar}. \tag{35b}$$

In the analysis for $\vec{B}$, we have not included exchange-polarization and correlation effects as we did for the isotropic term A. Since the free nitrogen atom is spherically symmetric, such effects are absent and so we do not have available the requisite diagrams for the free atom which could be adjusted to obtain the isotropic contributions in the pseudo-atom. However, an analysis of these anisotropic core-hyperfine effects in the excited p-state alkali atoms [21, 22] indicates that such effects are usually no more than ten percent of the direct effect. It is unlikely that anisotropic core hyperfine effects in our nitrogen pseudo-atom would have any more relative importance than this and so their neglect is not very serious.

Adding the isotropic hyperfine constant (1.82 gauss, Table 4) to the dipolar contributions (Eq. 35 b) we find that the hyperfine splittings predicted along the principal axes of hemin are: $X = 0.893$ gauss, $Y = 3.211$ gauss, $Z = 1.357$ gauss. Thus the MO calculation predicts a highly anisotropic hyperfine pattern, in contrast to the nearly isotropic splitting observed by Scholes [4] in single crystals, where a hyperfine splitting of $3.1 \pm \sim 0.3$ gauss was found. As can be seen from Table 1, the calculation predicts large differences in the populations of p_x, p_y and p_z on nitrogen and it is these differences which give rise to predicted anisotropic hyperfine coupling. The Scholes [4] experimental result suggests that all the unpaired populations in the nitrogen orbitals are small, or that they are all very nearly equal. In either case small dipolar hyperfine would be the result. We feel it most likely that the $d_{x^2-y^2} - p_y$ interaction has been overestimated relative to the $d_{xy} - p_x$ and $d_{yz} - p_z$ interactions. This could happen if, for example the $d_{x^2-y^2} - p_y$ overlap integral is too large relative to $d_{xy} - p_x$ or $d_{yz} - p_z$. Since we used single term Slater functions in the overlap calculations, such errors could arise. An improvement of the method would therefore involve calculation of Fe-N overlap integrals with an extended basis set-for example Clementi's functions [11]. Another possibility is that the $d_{x^2-y^2}$ orbital is "contracted" in the molecule due to repulsion by nitrogen lone pair electrons. This would effectively lower the $d_{x^2-y^2}$ interaction. It is interesting to observe here that just such a contraction is what is required to improve our earlier calculation of the quadrupole splitting at iron [1], where the correct magnitude but wrong sign was obtained. We now find that a preliminary examination of the situation indicates that a slight contraction of $d_{x^2-y^2}$ relative to the other d-orbitals could lead to a positive contribution to the coupling constant which could offset the negative result we had found earlier and produce the correct sign and order-of-magnitude of the field gradient at iron. It thus appears that the limited basis set MO method is not flexible enough for calculation of certain hyperfine parameters.

Nuclear Quadrupole Coupling

Both the magnetic dipole and electric quadrupole coupling constants depend on the asymmetry of the charge distribution in the neighborhood of nitrogen. But while the magnetic interaction depends only on the charge density due to the surplus spin states, the quadrupole interaction involves the entire density. Thus these two hyperfine interactions provide complementary information regarding the electronic structure of hemin.

The nuclear electric quadrupole Hamiltonian in the principal axis system of the field-gradient tensor, components $q_{x''x''}$, $q_{y''y''}$, $q_{z''z''}$, may be expressed in the form [23]:

$$\mathscr{H}_Q = \frac{e^2 Q q_{z''z''}}{4I(2I-1)}[(3I_{z''}^2 - \boldsymbol{I}\cdot\boldsymbol{I}) + \eta(I_{x''}^2 - I_{y''}^2)] \tag{36}$$

where

$$|q_{z''z''}| \geqq |q_{y''y''}| \geqq |q_{x''x''}| \,. \tag{37}$$

The asymmetry parameter, η, is given by

$$\eta = \frac{q_{x''x''} - q_{y''y''}}{q_{z''z''}} \,. \tag{38}$$

We shall make use the definition of the field-gradient tensor operator in the form:

$$q_{kl}^{\text{op.}} = -\sum_{\substack{i \\ \text{all valence} \\ \text{electrons}}} \frac{\partial^2\left(\frac{1}{r_i}\right)}{\partial\chi_{ki}\partial\chi_{li}} \tag{39}$$

where x_{ki} are x, y, or z ($k = 1$, 2, or 3) coordinates of the i^{th} electron in the molecular axis system. The field-gradient tensor q_k in the molecular axis system can be obtained by taking the expectation value of the $q_k^{\text{op.}}$ over the entire molecular wave-function including all valence electrons. The sum over electrons in the operator in Eq. (39) then gets replaced by a sum of expectation values over all the occupied MO functions ψ_μ. On substituting for ψ_μ from Eq. (1) in terms of atomic orbitals φ_n,

$$q_{kl} = \sum_{\substack{\mu=1 \\ \left(\text{all occupied} \atop \text{MO's}\right)}}^{66} \sum_{\substack{m,n \\ \left(\text{over all} \atop \text{AO's}\right)}} c_{\mu m} c_{\mu n} \langle \varphi_m | q_{kl}^{\text{op.}} | \varphi_n \rangle \, n(\mu) \tag{40}$$

where $n(\mu) = 1$ and 2 for singly and doubly occupied orbitals. Again in view of the $1/r^3$ dependence of the $q_k^{\text{op.}}$, the non-local and distant terms would be expected to be small [20]. However this neglect is somewhat less justified than for the magnetic dipolar case, due to antishielding effects [24]. But in the absence of a definite knowledge of these antishielding factors, particularly for the non-local terms, we have neglected the non-local and distant terms rather than introduce uncertainties. Hopefully such effects can be evaluated in the future and added to our results here. Our earlier calculation of the quadrupole splitting at iron [1] also considered only local terms. The calculated value of ΔE was -0.73 mm/sec, while the experimental Mössbauer data of Johnson [32] for hemin chloride seems best fit by $\Delta E = +0.76$ mm/sec. We therefore may have obtained the wrong calculated sign of ΔE. A more detailed calculation of ΔE at iron, which includes non-local and distant terms, as well as possible d-orbital expansion and contraction effects, is being carried out.

Here we only consider local terms for nitrogen, which in effect corresponds to applying the Townes and Dailey theory [25], except that our atomic populations

are obtained from MO calculations rather than from empirical estimates of ionic characters and hybridization parameters.

$$\vec{q} = -\left\langle \frac{1}{r^3} \right\rangle_{2p} \sum_{\mu=1}^{66} n(\mu) \begin{pmatrix} \frac{2}{5}(2c_{\mu x}^2 - c_{\mu y}^2 - c_{\mu z}^2) & \frac{6}{5} c_{\mu x} c_{\mu y} & \frac{6}{5} c_{\mu x} c_{\mu z} \\ \frac{6}{5} c_{\mu y} c_{\mu x} & \frac{2}{5}(2c_{\mu y}^2 - c_{\mu z}^2 - c_{\mu x}^2) & \frac{6}{5} c_{\mu y} c_{\mu z} \\ \frac{6}{5} c_{\mu z} c_{\mu x} & \frac{6}{5} c_{\mu z} c_{\mu y} & \frac{2}{5}(2c_{\mu z}^2 - c_{\mu x}^2 - c_{\mu y}^2) \end{pmatrix} \tag{41a}$$

Substituting for $\langle r^{-3} \rangle_{2p}$ and for $c_{\mu x}$, $c_{\mu y}$ and $c_{\mu z}$ from our molecular orbital calculations we get

$$\vec{q} = \begin{pmatrix} 0.9731 & 0.0 & 0.0 \\ 0.0 & -0.5969 & -0.1018 \\ 0.0 & -0.1018 & -0.3762 \end{pmatrix} a_0^{-3}. \tag{41b}$$

The diagonalization of the $\vec{q}$ tensor is achieved by an identical procedure as for the $\vec{B}$ tensor. The principal axis system for $\vec{q}$ is obtained by a rotation of the molecular coordinate system by $+21.36°$ around the molecular x-axis (see Fig. 1). In order to conform with the convention in Eq. (37), we redefine the principal axes of $\vec{q}$ such tnat x and z axes after the rotation are interchanged and y is replaced by $-y$. The principal axes chosen in this way are relabeled with double primes, the principal components being given by:

$$\vec{q}''_{\text{tot}} = \begin{pmatrix} -0.2673 & 0.0 & 0.0 \\ 0.0 & -0.7058 & 0.0 \\ 0.0 & 0.0 & +0.9731 \end{pmatrix}. \tag{42}$$

The two essential parameters that define the field-gradient tensor in the principal axis system are $q_{z''z''} = +0.9731\, a_0^{-3}$, and $\eta = 0.457$. For the sake of analysis of the relative importance of the paired and unpaired electron states in determining the field-gradient, we have separated these contributions to $\vec{q}$ and listed them in Eqs. (43) and (44). The two contributions are separately diagonalized, the principal axes of $\vec{q}_{\text{unpaired}}$ being identical to those of the $\vec{B}$ tensor while $\vec{q}_{\text{paired}}$ requires a rotation of $\theta_{\vec{q},\text{paired}} = 16.36°$ about the molecular x-axis followed by a similar relabeling as for $\vec{q}_{\text{tot}}$:

$$\vec{q}_{\text{unpaired}} = \begin{pmatrix} 0.1685 & 0.0 & 0.0 \\ 0.0 & 0.3374 & 0.0 \\ 0.0 & 0.0 & -0.5059 \end{pmatrix} a_0^{-3}, \tag{43}$$

$$\vec{q}_{\text{paired}} = \begin{pmatrix} -0.0094 & 0.0 & 0.0 \\ 0.0 & -0.6383 & 0.0 \\ 0.0 & 0.0 & +0.6477 \end{pmatrix} a_0^{-3}. \tag{44}$$

It is noteworthy that $\vec{q}_{\text{unpaired}}$ at the ligand nitrogen nucleus is sizeable, in keeping with the substantial degree of mixing of metal and ligand orbitals observed in the analysis of the isotropic hyperfine constant. Also the paired

orbitals are found to make a major contribution to the field-gradient tensor, indicating that there, as in the case of the Fe^{57m} nucleus [1], no simple relation is expected between $\vec{q}_{\text{tot}}$ and $\vec{B}$. We should note here that the $\vec{q}_{\text{unpaired}}$ is probably no better calculated than was $\vec{B}$, since both quantities depend upon the same electron distribution (see above for difficulties with the $\vec{B}$ calculation). We have no way of assessing the accuracy of $\vec{q}_{\text{paired}}$, because there is no experimental separation of $\vec{q}_{\text{unpaired}}$ and $\vec{q}_{\text{paired}}$. Further discussion is not warranted in the absence of the necessary experimental quadrupole data.

In order to calculate the quadrupole coupling constant, e^2Qq defined by

$$e^2Qq = e^2Q(1-\gamma)\, q_{z''z''}\,. \tag{45}$$

We require a knowledge of both Q and the atomic shielding factor γ. Neither of these quantities is known definitely. Values of Q in the literature for example range from [26, 27] $Q = 0.007 \times 10^{-24}\,\text{cm}^2$ to $0.03 \times 10^{-24}\,\text{cm}^2$. The reason for this is that no atomic measurements which yield Q more accurately are available since nitrogen is spherically symmetric in its ground-state (^4S) and the values quoted are derived from estimates of the field-gradients in molecules.

In order to avoid these uncertainties, we have made use of the coupling constant $(e^2Qq)_p \approx -9$ mc/sec per p-electron that seems to fit most available data in nitrogen compounds [28] and combine it with the MO calculations to yield

$$\begin{aligned} e^2Qq &\approx e^2Qq_p \sum_{\mu=1}^{66} \left(c_{\mu z''}^2 - \frac{c_{\mu x''}^2 + c_{\mu y''}^2}{z} \right) n(\mu) \\ &= -\frac{5q_{z''z''}}{4\langle r^{-3}\rangle_{2p}}\, e^2Qq_p \\ &= +3.575\ \text{mHz} \end{aligned} \tag{46}$$

with $q_{z''z''} = +0.9731\, a_0^{-3}$ and $\langle r^{-3}\rangle_{2p} = 3.0996\, a_0^{-3}$.

If we had made use of Eq. (45), it would be necessary to incorporate shielding effects of the core-electrons on the field-gradient due to the valence electrons at the nucleus and also the influence of correlation effects [21]. Similar comments regarding these corrections would apply here as in the case of $\vec{B}$ since both of these properties involve similar angular dependence on electronic coordinates. However, by utilizing an empirical value of e^2Qq_p, we are indirectly incorporating shielding and correlation effects. The extent to which such effects have been included will depend on the validity and accuracy of the choice for e^2Qq_p.

It would be very interesting to compare our prediction with the experimental values of e^2Qq and η when available as another test of the predictions of the MO theory used here for hemin.

Conclusion

As remarked earlier, while the major part of the isotropic nitrogen hyperfine constant arises from the direct effect, the exchange-polarization contribution was also found to be important from a quantitative point of view. For purposes of discussion it is helpful to split up the exchange-polarization effect into two parts,

a part arising from the 1s core and the other from the paired valence electrons. The former is probably quite well estimated by our adaptation of Brueckner-Goldstone technique. However, the need to use the Mulliken approximation in this case could have been avoided if we had utilized the moment-perturbation approach [19] and calculated the exchange interaction using the actual unpaired orbitals rather than the pseudo-atom approximations. The second contribution, that from the paired valence orbital cannots, be simply evaluated by the moment-perturbation technique, because of the multicenter nature of the paired valence orbitals. This contribution can however be evaluated alternatively by a molecular orbital approach of the UHF type. The recent work of Pople using the INDO method [18] would be helpful in this respect. However, to incorporate correlation effects in an approach of this type one would have to utilize configuration interactions [29] which complicate the calculation and require a careful choice of configurations that have to be admixed. Our adaptation of the Brueckner-Goldstone procedure for atoms through the pseudo-atom procedure thus provides a viable alternative for an estimation of the contribution from many-body effects.

Both the isotropic and anisotropic magnetic hyperfine constant for the N^{14} nucleus have been found to be quite substantial. A crystal field model [5], which presumes essential localization of the unpaired electrons on the iron, would be quite inadequate to explain the substantial N^{14} hyperfine interaction. The interpretation of optical data [2], the Fe^{57m} magnetic and quadrupole hyperfine interactions [1] and the proton shifts [31] observed by NMR also argue against the crystal field model and favor the delocalized molecular orbital picture.

The molecular orbital model is not without fault, however. This method seriously over-estimates the anisotropic (dipolar) hyperfine interaction, at the same time giving the wrong calculated sign of the quadrupole splitting at iron [1]. It is, therefore, felt that better MO methods must be found, or that the extended Hückel method must be made more flexible by allowing the atomic orbitals to distort.

Since the N^{14} quadrupole interaction derives contributions from both paired and unpaired orbitals, it is perhaps a less sensitive index of the conjugation between the iron and porphyrin orbitals. The magnitude of the quadrupole coupling constant is rendered a little uncertain by the uncertainties in the N^{14} quadrupole moment. Perhaps it would be more meaningful to compare theoretical and experimental results (when the latter are available) in terms of the ratio of e^2Qq in hemin and other nitrogen compounds such as pyrrole and pyridine. In addition, experimental information on the asymmetry parameter, η, and the orientation of the principal axes, which are independent of Q, would be very desirable to have for comparison with theory.

A theoretical calculation is currently in progress for the relatively large zero-field splitting term in the spin-Hamiltonian of hemin, which has been measured experimentally [32]. When experimental data are available to test our prediction for N^{14} hyperfine structure, hemin will have the status of being unique among the simpler of the biologically important molecules whose electronic structure have been subjected to detailed quantitative analysis in analyzing the wealth of microscopic properties available by current advances in physico-chemical experimental techniques.

References

1. Rettig, M. F., Han, P. S., Das, T. P.: Theoret. chim. Acta (Berl.) **12**, 178 (1968). See also "Erratum", Theoret. chim. Acta (Berl.) **13**, 432 (1969).
2. Zerner, M., Gouterman, M., Kobayashi, H.: Theoret. chim. Acta (Berl.) **6**, 636 (1966) and references therein.
3. Pullman, B., Spanjaard, C., Berthier, G.: Proc. Nat. Acad. Sci. USA **46**, 1011 (1960).
4. After this work was completed and submitted for publication, Scholes, C. P.: Proc. Nat. Acad. Sci. **62**, 428 (1969), reported esr results for hemin and hematin which revealed nitrogen hyperfine structure for the first time in this type of molecule.
4. a) Orgel, L. E.: I.U.B. Symposium Series **19**, 1—13 (1961); b) Griffith, J. S.: Proc. Roy. Soc. A **235**, 23—36 (1956); Nature **180**, 30—31 (1957); Disc. Faraday Soc. **26**, 81—86 (1958); c) Harris, G.: J. chem. Physics **48**, 2191 (1968); Theoret. chim. Acta (Berl.) **5**, 379 (1966); Theoret. chim. Acta (Berl.) **10**, 119 (1968); Theoret. chim. Acta (Berl.) **10**, 155 (1968).
6. Dutta, N. C., Matsubara, C., Pu, R. T., Das, T. P.: Physic. Rev. **177**, 33 (1969).
7. Chang, E. S., Pu, R. T., Das, T. P.: Physic. Rev. **174**, 1 (1969).
8. Hoffmann, R., Lipscomb, W. N.: J. chem. Physics **36**, 2179 (1962).
9. Rettig, M. F., Drago, R. S.: J. Amer. chem. Soc. **91**, 3432 (1969).
10. Wolfsberg, M., Helmholz, L.: J. chem. Physics **20**, 837 (1952).
11. Clementi, E.: Tables of atomic functions, I.B.M. Corporation, 1965.
12. Mulliken, R. S.: J. chem. Physics **23**, 1833 (1955).
13. — J. chem. Physics **23**, 1841 (1955).
14. Ramsey, N. F.: Nuclear moments. New York: John Wiley and Sons, Inc. 1953.
15. Heine, V.: Physic. Rev. **107**, 1002 (1957).
16. Anderson, L. W., Pipkin, F. M., Baird, J. C.: Physic. Rev. **116**, 87 (1959).
17. a) Snyder, L. C., Amos, T.: J. chem. Physics **42**, 3670 (1965); b) Bagus, P. S., Liu, B.: Physic. Rev. **148**, 79 (1966); c) Amos, A. T., Davison, S. G.: Molecular Physics **10**, 261 (1966); d) Hinchliffe, A.: Theoret. chim. Acta (Berl.) **5**, 451 (1966).
18. Pople, J. A., Beveridge, D. L., Dobosh, P. A.: J. Amer. chem. Soc. **90**, 4201 (1968).
19. Gaspari, G. D., Shyu, Wei-Mei, Das, T. P.: Physic. Rev. **134**, A 852 (1964).
20. Ikenberry, D., Das, T. P.: J. chem. Physics **45**, 1361 (1966).
21. Lyons, J. D., Pu, R. T., Das, T. P.: Physic. Rev. (In press).
22. Sternheimer, R. M.: Physic. Rev. **84**, 244 (1951).
23. Das, T. P., Hahn, E. L.: Nuclear quadrupole resonance spectroscopy, New York: Academic Press, Inc. 1958.
24. —, Karplus, M.: J. chem. Physics **30**, 848 (1959).
25. Townes, C. H., Dailey, B. P.: J. chem. Physics **17**, 782 (1949); Schempp, E., Bray, P. J.: J. chem. Physics **46**, 1186 (1967); **48**, 2381 (1968); Physics Letters **25** A, 414 (1967).
26. Bassompierre, A.: Disc. Faraday Soc. **19**, 260 (1955); Sheridan, J., Gordy, W.: Physic. Rev. **79**, 513 (1950).
27. Kisliuk, P. J.: J. chem. Physics **22**, 86 (1954).
28. Lucken, E. A. C.: Review talk at summer school on nuclear quadrupole resonance spectroscopy, Frascati (Rome), Italy, 11—21 October (1967). Sponsored by University of Frankfurt, Germany and North Atlantic Treaty Organization.
29. Moss, R. E.: Molecular Physics **10**, 501 (1966).
30. Shulman, R. G., Wüthrich, K., Yamane, T., Ogawa, S.: 13th Annual Meeting of the Biophysical Society, Los Angeles, February 26–March 1, 1969.
31. Richards, P. L., Caughey, W. S., Eberspaecher, H., Feher, G., Malley, M.: J. chem. Physics **47**, 1187 (1967).
32. Johnson, C. E.: Physics Letters **21**, 419 (1966).

Professor P. S. Han
Department of Physics
Air Force Academy
Daebang-Dong, Yong Doong po-Ku
Seoul, Korea

Professor T. P. Das
Department of Physics
University of Utah
Salt Lake City, Utah 84112, USA

Professor M. F. Rettig
Department of Chemistry
University of California
Riverside, California 92502, USA